

Journal Pre-proofs

Research paper

Decomposition of Ammonia on $\text{ZrB}_2(0001)$

Weronika Walkosz, Kedar Manandhar, Michael Trenary, Peter Zapol

PII: S0009-2614(19)30965-0

DOI: <https://doi.org/10.1016/j.cplett.2019.136984>

Reference: CPLETT 136984

To appear in: *Chemical Physics Letters*

Received Date: 14 August 2019

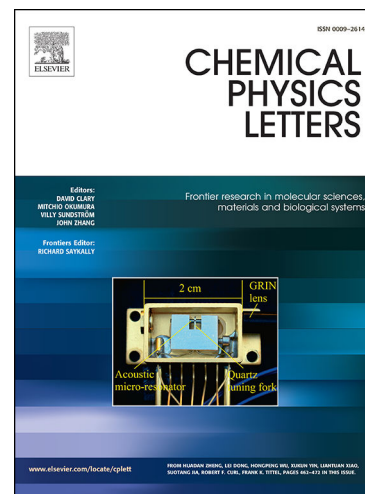
Revised Date: 18 November 2019

Accepted Date: 23 November 2019

Please cite this article as: W. Walkosz, K. Manandhar, M. Trenary, P. Zapol, Decomposition of Ammonia on $\text{ZrB}_2(0001)$, *Chemical Physics Letters* (2019), doi: <https://doi.org/10.1016/j.cplett.2019.136984>

This is a PDF file of an article that has undergone enhancements after acceptance, such as the addition of a cover page and metadata, and formatting for readability, but it is not yet the definitive version of record. This version will undergo additional copyediting, typesetting and review before it is published in its final form, but we are providing this version to give early visibility of the article. Please note that, during the production process, errors may be discovered which could affect the content, and all legal disclaimers that apply to the journal pertain.

© 2019 Published by Elsevier B.V.



Decomposition of Ammonia on ZrB₂(0001)

Weronika Walkosz^{1,2}, Kedar Manandhar³, Michael Trenary³, Peter Zapol¹

¹Materials Science Division, Argonne National Laboratory, 9700 S. Cass Ave., Argonne, IL 60439

²Department of Physics, Lake Forest College, 555 N. Sheridan Rd., Lake Forest, IL 60045

³Department of Chemistry, University of Illinois at Chicago, 845 W Taylor Street, Chicago, IL 60607

Abstract

Zirconium diboride has been recently identified as a promising substrate for the growth of Group-III nitride semiconductors using reactive vapors that include ammonia as the nitrogen source. Adsorption energies and dissociation pathways of NH₃ on the (0001) surface of ZrB₂ were investigated using density functional theory calculations. Our results indicate that NH₃ readily adsorbs onto the ZrB₂ surface terminated with Zr and decomposes to atomic N and H with relatively small activation barriers. The resulting atomic species are found to be mobile with the computed diffusion barriers between 0.11 and 0.78 eV.

Keywords: ZrB₂; Group-III nitrides; GaN; NH₃ adsorption; DFT

1. Introduction

Group-III nitride semiconductors (GaN, InN, and AlN), have emerged as key materials for applications in visible and UV optoelectronics and in high-power and high-frequency electronics because of their tunable band gaps, high radiation hardness, and good thermal stability. Despite the remarkable progress in the commercialization of nitride-based devices, the lack of lattice-matched substrates for the growth of high quality nitride films still remains a technological challenge. A high defect density and biaxial strain due to the heteroepitaxial growth on foreign substrates such as α -Al₂O₃, SiC, Si, ZnO, lead to grain boundaries, threading dislocations, stacking faults, and strong, built-in electrostatic

fields, all limiting device performance and reliability. Therefore, the identification of lattice- matched substrates for epitaxial growth of group-III nitride films is highly desirable.

Kinoshita *et al.* have reported the synthesis of electrically conductive single crystals of ZrB_2 and proposed their use as substrates for the epitaxial growth of GaN.¹ The crystal structure of ZrB_2 is simple hexagonal with the lattice constants $a = 3.169 \text{ \AA}$ and $c = 3.530 \text{ \AA}$, the former being only 0.63 % larger than that of wurtzite GaN ($a = 3.189 \text{ \AA}$).² The thermal expansion coefficient of ZrB_2 along $[10\bar{1}0]$ on the basal plane is $5.9 \times 10^{-6} \text{ K}^{-1}$, which is also very close to that of GaN ($5.6 \times 10^{-6} \text{ K}^{-1}$). This outstanding structural and thermal match between the two materials has led to high quality GaN films grown on ZrB_2 substrates by pulsed laser deposition (PLD).³ Promising outcomes have also been reported for the films grown by molecular beam epitaxy (MBE) and metal organic chemical vapor deposition (MOCVD), the latter being commonly used for the production of device-quality nitride films.^{4,5} However, in the case of MOCVD growth, a low temperature buffer layer was necessary to prevent the substrate's complete nitridation. In this technique, growth occurs via gas phase and surface chemical reactions involving gallium and nitrogen containing precursors, such as trimethyl gallium and ammonia, respectively. Surface decomposition and diffusion reactions are thought to govern the growth, but their characterization is still lacking. A detailed quantification and understanding of the kinetics of precursor decomposition on the $ZrB_2(0001)$ surface is important for the controlled growth of GaN on the ZrB_2 substrates by MOCVD. While most of the computational and experimental studies on ZrB_2 have focused on its bulk properties,⁶⁻²⁰ several studies investigated the $ZrB_2(0001)$ surface. Computationally, structure and bonding features of the bare and oxygenated $ZrB_2(0001)$ surface were investigated with density functional theory (DFT).²¹⁻²³ Experimentally, the $ZrB_2(0001)$ surface subjected to thermal cleaning up to 1000° C in vacuum as well as to the treatment in HF aqueous solution was studied with X-ray photoelectron spectroscopy (XPS), reflection high-energy electron diffraction (RHEED), and atomic force microscopy (AFM).²⁴ Surface phonon dispersion of $ZrB_2(0001)$ was measured with high-resolution electron energy loss spectroscopy (HREELS).^{25,26} Aizawa *et al.* also studied the adsorption of H_2 , 2H_2 , O_2 and CO on the $ZrB_2(0001)$ surface using the same technique.²⁷ The oxidation of $ZrB_2(0001)$ at high

temperature was studied using reflection high-energy electron diffraction, Auger electron spectroscopy, HREELS, and XPS²⁸ as well as DFT.²⁹ The surface and interface energies of GaN(0001) on ZrB₂(0001) were calculated with DFT.^{30,31} Recently, we reported a combined DFT, XPS, and reflection adsorption infrared spectroscopy (RAIRS) study of the adsorption of hydrogen and ammonia onto the (0001) surface of ZrB₂.³²⁻³⁴ Our results have indicated that the surface reacts with H and also facilitates NH₃ dissociation. We also studied the dissociation of trimethylgallium on the ZrB₂(0001) surface using X-ray photoelectron spectroscopy and RAIRS.³⁵ In this work, we perform a detailed investigation of NH₃ adsorption and decomposition pathways on the Zr-terminated (0001) surface of ZrB₂ using DFT. We report adsorption geometries and energies, transition states, intermediates, and activation barriers for the elementary decomposition reactions. The results are discussed in the context of the MOVPE growth mechanism of GaN on ZrB₂ substrates, and provide the basis for chemical kinetic models for more controlled nitride growth. Kinetic models based on DFT parametrization were successfully used in the past for the prediction of structure, properties, and reactivity of various materials.³⁶⁻³⁸ The rest of the paper is organized as follows. In the next section, we provide details of the computational methods used in this work. The results and the discussion of the adsorption geometries and energies as well as NH₃ decomposition barriers are presented in Sections 3 and 4. We conclude with a brief discussion and summary in Sections 5 and 6, respectively.

2. Computational Details

The ab-initio density functional theory (DFT) calculations were performed using the projector augmented wave (PAW) method in the VASP implementation.^{39,40} The exchange-correlation interaction was treated with the generalized gradient approximation in the parameterization of Perdew, Burke, and Ernzerhof (PBE). A cutoff energy of 400 eV and a (4×4×1) Monkhorst-Pack grid were used for geometry optimizations. We focused on the Zr-terminated (0001) surface as it has been shown to be more stable than the B-terminated surface²¹ as expected for Group IV metals.⁴¹ The surface calculations were performed with the optimized lattice parameters ($a = 3.179 \text{ \AA}$ and $c = 3.548 \text{ \AA}$) using a symmetric slab with a (2×2) surface unit cell consisting of seven atomic layers of

ZrB₂. The optimized lattice parameters are in good agreement with the experimental^{2,42} and other theoretically calculated results.^{10,13,21} The vacuum layer size was ~ 17 Å in the direction normal to the surface. Only one side of the slab was used for adatom adsorption. Activation and diffusion barriers were calculated using the climbing image nudged elastic band method.⁴³ The adsorbate binding energies (BE) were calculated using the relation

$$BE = E_{surf+adsorb} - E_{surf} - E_{adsorb}$$

where $E_{surf+adsorb}$ is the total energy of the surface with the adsorbed species, E_{surf} is the total energy of the bare (relaxed) surface, E_{adsorb} is the total energy of gas phase NH₃, NH₂, NH, H, or N. The latter were calculated by placing the molecules in asymmetric ($10 \times 11 \times 12$ Å) cells. A negative value of BE implies an energetically favored adsorption process.

3. Adsorption Sites and Energies

Geometry optimizations have been performed for NH₃, NH₂, NH, N, and H at different adsorption sites on the ZrB₂(0001) surface shown in Figure 1. Table 1 lists the calculated BE for the adsorbates at their most favorable sites while the optimized structures are shown in Figure 1. Ammonia adsorbs dissociatively on the Zr-terminated surface of ZrB₂, with the Zr site being a transition state site. The BE of NH₃ at this site is -0.95 eV and the N-Zr and N-H bond lengths are 2.38 Å and 1.03 Å, respectively. The three H-N-H angles are 109.21°. For comparison, the calculated intermolecular parameters of an isolated NH₃ molecule are 1.03 Å and 107.12°. We note here that we tested different rotational conformers for the initial positions of NH₃ on the diboride surface. As for NH₂, its most favorable site corresponds to the threefold hollow site between three surface Zr atoms with the BE of -4.30 eV. In this configuration, the NH₂ C₂-axis is perpendicular to ZrB₂(0001) and the H atoms point to the bridge and Zr sites. The calculated N-Zr bonds are 2.34, 2.42 and 2.42 Å, and the N-H bonds are 1.04 and 1.05 Å. The H-N-H angle is 102.66°. These parameters are similar to those of the gas phase NH₂ molecule (1.04 Å and 102.71°) calculated with DFT. Similarly to NH₂, the adsorption of NH is also the most favorable at the threefold hollow site with a BE of -6.78 eV and the three Zr-N and one

N-H bonds of 2.22 Å and 1.03 Å in length, respectively. The calculated N-H bond of NH in gas phase was found to be 1.06 Å in length. Lastly, the adsorption configurations of N and H correspond to the threefold hollow sites with the *BEs* of -2.72 and -1.14 eV calculated with respect to atomic N and H, respectively. The N atom sits 2.96 Å above the subsurface B atom and it makes three bonds of 2.10 Å with the surrounding surface Zr atoms, whereas the H atom is 2.85 Å above the subsurface B and the Zr-H bonds are 2.15 Å in length. Comparing the species, the adsorption energies of NH_x (x = 1-3) become more negative when the number of H atoms decreases, while the molecules make shorter bonds with the surface Zr atoms. This indicates a stronger interaction of the dehydrogenated species with the surface. Similar trends were reported for NH_x (x = 1-3) on metallic surfaces.⁴⁴⁻⁴⁷

4. Reaction Pathways for Decomposition of Ammonia

Dehydrogenation reactions for the complete decomposition of NH₃ on the ZrB₂(0001) surface were studied in detail, with the product states of the reactions determined based on the stability of the NH_x species and the calculated activation barriers for each dehydration step. As stated in the previous section, the adsorption of ammonia onto the bare ZrB₂(0001) surface results in its decomposition to NH₂ and H at two non-neighboring hollow sites, thus reducing the electrostatic repulsion between the two moieties. The reaction is exothermic by 1.93 eV. In the second dissociation reaction, the adsorbed NH₂ molecule initially at the hollow site decomposes to NH and H at the two non-neighboring hollow sites. At the transition state geometry, the N-H bond is stretched to 1.33 Å. The barrier for this reaction is 0.23 eV and the process is exothermic by 1.52 eV. For NH dehydrogenation, the initial state corresponds to the NH molecule at the hollow site, while the final state consists of N and H at two non-neighboring hollow sites. At the transition state, the N-H bond is stretched to 1.42 Å. The activation barrier for this reaction is 1.37 eV and the process is exothermic by 0.17 eV.

5. Discussion

To compare the reaction energies of the dehydrogenation steps discussed above, we referenced their adsorption energies to the NH_3 molecule in the gas phase. Figure 2 shows the calculated reaction pathway for the complete decomposition of NH_3 at $T = 0$ K. In each step, the initial state is an NH_{3-x} ($x = 0-2$) species and x adsorbed H atoms without lateral interactions, while the final state corresponds to the NH_{3-x-1} species and one H atom co-adsorbed on the same (2×2) surface unit cell and x adsorbed H atoms at large separation. The pathway shows that the first two dehydrogenation steps, namely NH_3 and NH_2 decompositions to yield NH and H, are both kinetically and thermodynamically facile as their barriers are small and they are exothermic. Further decomposition to N and H has a significantly larger barrier (1.37 eV) and can be assumed to be the rate limiting step in the complete decomposition of NH_3 on $\text{ZrB}_2(0001)$. However, the reaction is exothermic, thus favorable from the thermodynamic considerations. In fact, the whole decomposition process is thermodynamically favorable and there is no apparent barrier. Moreover, we find that the resulting moieties are fairly mobile, thus no significant energy needed to overcome decomposition barriers is expected to be lost due to their surface diffusion. The calculated barriers for NH_2 , NH , N, and H migration between their stable sites are 0.11, 0.46, 0.78, and 0.27 eV respectively.³² This implies that the complete decomposition of NH_3 to atomic N and H should ensue, especially at higher temperatures required for the MOCVD growth of Group-III nitrides. Although N deposition through NH_3 decomposition on $\text{ZrB}_2(0001)$ is a vital step in the nitride growth, previous work has shown that at high temperatures the surface becomes nitrated. The control of this process is a key to the growth of high-quality nitride films.

The prediction of complete dissociation of NH_3 on $\text{ZrB}_2(0001)$ was recently verified by our recent XPS and RAIRS experiments for temperatures of 300 K and above.³⁴ However, the measurements have indicated that hydrogen-bonded clusters with the same structure as solid ammonia are formed on the diboride surface at lower temperatures. In this work, only one molecule per (2×2) surface unit cell was studied, thus no hydrogen bonding interactions were allowed. A deeper understanding of the atomic structures of the diboride surface in the ammonia environment will naturally require chemical kinetic models based on the ab initio calculations presented in this paper, incorporating more NH_3 molecules and using larger surface unit cells.

6. Conclusions

Density functional theory calculations have been performed for the adsorption and decomposition of NH_3 on the Zr-terminated (0001) surface of ZrB_2 . We have predicted the adsorption sites, geometries, as well as the relative stabilities of the adsorbed ammonia and its dehydrogenated species. Our calculations show NH_3 readily adsorbs onto the Zr-site of the diboride surface and it dissociates to atomic N and H with relatively small activation barriers. The largest activation barrier corresponded to the NH decomposition. The complete dissociation of NH_3 was found to be exothermic, thus favorable from the thermodynamic considerations. Moreover, the resulting decomposition moieties were shown to be very mobile on the diboride surface.

Acknowledgements

This work was supported by the U. S. Department of Energy, Office of Science, Office of Basic Energy Sciences-Division of Materials Sciences and Engineering under Contract No. DE-AC02-06CH11357. M.T. acknowledges partial support from the National Science Foundation under grant CHE-1800236. We acknowledge grants of computer time from ANL Computing Resource Center (LCRC), ANL Center of Nanoscale materials (CNM), and the National Energy Research Scientific Computing Center (NERSC).

Bibliography

1. Kinoshita H, Otani S, Kamiyama S, et al. Zirconium diboride (0001) as an electrically conductive lattice-matched substrate for gallium nitride. *Jpn J Appl Phys* 2. 2001; 40(12A):L1280-L1282.
2. Powder diffraction file, Joint Committee of Powder Diffraction Standard (JCPDS) No. 34-423.
3. Kawaguchi Y, Kobayashi A, Ohta J, Fujioka H. Characteristics of GaN/ ZrB_2 heterointerfaces prepared by pulsed laser deposition. *Jpn J Appl Phys* 1. 2006;45(9A):6893-6896.

4. Suda J, Matsunami H. Heteroepitaxial growth of group-III nitrides on lattice-matched metal boride ZrB_2 (0001) by molecular beam epitaxy. *J Cryst Growth*. 2002; 237:1114-1117.
5. Tomida Y, Nitta S, Kamiyama S, et al. Growth of GaN on ZrB_2 substrate by metal-organic vapor phase epitaxy. *Appl Surf Sci*. 2003; 216(1-4):502-507.
6. Fuchs G, Drechsler SL, Muller KH, et al. A comparative study of MgB_2 and other diborides. *J Low Temp Phys*. 2003; 131(5-6):1159-1163.
7. Wang XB, Tian DC, Wang LL. The Electronic-Structure and Chemical-Stability of the AlB_2 -Type Transition-Metal Diborides. *J Phys-Condens Mat*. 1994; 6(46):10185-10192.
8. Fahrenholtz WG, Hilmas GE, Talmy IG, Zaykoski JA. Refractory diborides of zirconium and hafnium. *J Am Ceram Soc*. 2007; 90(5):1347-1364.
9. Vajeeston P, Ravindran P, Ravi C, Asokamani R. Electronic structure, bonding, and ground-state properties of AlB_2 -type transition-metal diborides. *Phys Rev B*. 2001; 63(4):045115.
10. Fu HZ, Lu Y, Liu WF, Gao T. Pressure effects on elastic and thermodynamic properties of ZrB_2 . *J Mater Sci*. 2009; 44(20):5618-5626.
11. Huerta L, Duran A, Falconi R, Flores M, Escamilla R. Comparative study of the core level photoemission of the ZrB_2 and ZrB_{12} . *Physica C*. 2010; 470(9-10):456-460.
12. Zhang MG, Wang H, Wang HB, Zhang XX, Iitaka T, Ma YM. First-Principles Prediction on the High-Pressure Structures of Transition Metal Diborides (TMB_2 , $TM = Sc, Ti, Y, Zr$). *Inorg Chem*. 2010; 49(15):6859-6864.
13. Li H, Zhang LT, Zeng QF, et al. Crystal structure and elastic properties of ZrB compared with ZrB_2 : A first-principles study. *Comp Mater Sci*. 2010; 49(4):814-819.
14. Middleburgh SC, Parfitt DC, Blair PR, Grimes RW. Atomic Scale Modeling of Point Defects in Zirconium Diboride. *J Am Ceram Soc*. 2011; 94(7):2225-2229.
15. Kumar R, Mishra MC, Sharma BK, et al. Electronic structure and elastic properties of TiB_2 and ZrB_2 . *Comp Mater Sci*. 2012; 61:150-157.
16. Lawson JW, Daw MS, Bauschlicher CW. Lattice thermal conductivity of ultra high temperature ceramics ZrB_2 and HfB_2 from atomistic simulations. *J Appl Phys*. 2011; 110(8):083507.
17. Okamoto NL, Kusakari M, Tanaka K, Inui H, Yamaguchi M, Otani S. Temperature dependence of thermal expansion and elastic constants of single crystals of ZrB_2 and the suitability of ZrB_2 as a substrate for GaN film. *J Appl Phys*. 2003; 93(1):88-93.
18. Okamoto NL, Kusakari M, Tanaka K, Inui H, Yamaguchi M, Otani S. Mechanical and thermal properties of single crystals of ZrB_2 . *Defect Properties and Related Phenomena in Intermetallic Alloys*. 2003; 753:83-88.
19. Chen ZP, YS; Hu, M; Li, CM; Luo, YT. Elasticity, hardness, and thermal properties of ZrB_n ($n=1, 2, 12$). *Ceram Int*. 2016; 42(6):6624-6631.
20. Wang BZ, W; Li, WD. Mechanics, Lattice Dynamics, and Chemical Bonding in ZrB_2 and ZrB_{12} from First-Principles Calculations *Science of Advanced Materials*. 2013; 5(12):1916-1921(1916).

21. Zhang XH, Luo XG, Li JP, Han JC, Han WB, Hong CQ. Structure and bonding features of ZrB₂ (0001) surface. *Comp Mater Sci.* 2009; 46(1):1-6.
22. Cheng CL, HJ; Fu, QG. Initial oxidation of ZrB₂ (0 0 0 1) from first-principles calculations. *Comp Mater Sci.* 2018; 153:282-287.
23. Sun W, Liu J, Xiang H, Zhou Y. A Theoretical Investigation on the Anisotropic Surface Stability and Oxygen Adsorption Behavior of ZrB₂. *J Am Ceram Soc.* 2016; 99(12):4113 -4120.
24. Armitage R, Suda J, Kimoto T. Characterization of ZrB₂ (0001) surface prepared by ex situ HF solution treatment toward applications as a substrate for GaN growth. *Surf Sci.* 2006; 600(7):1439-1449.
25. Aizawa T, Hayami W, Otani S. Surface phonon dispersion of ZrB₂ (0001) and NbB₂ (0001). *Phys Rev B.* 2002; 65(2):024303.
26. Aizawa T, Suehara S, Hishita S, Otani S. Surface phonon dispersion of ZrB₂(0001)root 3 x root 3-B. *J Phys-Condens Mat.* 2008; 20(26):265006.
27. Aizawa T, Hayami W, Otani S. Adsorption of H-2, H-2(2), O-2, and CO on ZrB(0001). *J Chem Phys.* 2002; 117(24):11310-11314.
28. Aizawa T, Hishita S, Otani S. The 2 x 2 oxidized layer on ZrB₂(0001). *Appl Surf Sci.* 2009; 256(4):1120-1123.
29. Wang HK, Zhang X, Qiu XM. Adaptive smoothed molecular dynamics for multiscale modeling. *Comp Mater Sci.* 2009; 46(3):713-715.
30. Iwata JI, Shiraishi K, Oshiyama A. First-principle study on GaN epitaxy on lattice-matched ZrB₂ substrates. *Appl Phys Lett.* 2003; 83(13):2560-2562.
31. Liu P-L, Chizmeshya AVG, Kouvetakis J, Tsong IST. First-principles studies of GaN(0001) heteroepitaxy on ZrB₂ (0001). *Phys Rev B.* 2005; 72(24):245335.
32. Walkosz W, Manandhar K, Trenary M, Otani S, Zapol P. Dissociative adsorption of hydrogen on the ZrB₂ (0001) surface. *Surf Sci.* 2012; 606(23-24):1808-1814.
33. Manandhar K, Walkosz W, Trenary M, Otani S, Zapol P. Dissociative adsorption of ammonia on the ZrB₂ (0001) surface. *Surf Sci.* 2013; 615:110-118.
34. Manandhar K, Walkosz W, Ren Y, Otani S, Zapol P, Trenary M. Structure and Reactivity of Molecularly Adsorbed Ammonia on the ZrB₂ (0001) Surface. *J Phys Chem C.* 2014; 118(50):29260-29269.
35. Manandhar K, Trenary M, Otani S, Zapol P. Dissociation of trimethylgallium on the ZrB₂ (0001) surface. *J Vac Sci Technol A.* 2013; 31(6):061405.
36. Norskov JK, Bligaard T, Rossmeisl J, Christensen CH. Towards the computational design of solid catalysts. *Nat Chem.* 2009; 1(1):37-46.
37. Hansgen DA, Vlachos DG, Chen JG. Using first principles to predict bimetallic catalysts for the ammonia decomposition reaction. *Nat Chem.* 2010; 2(6):484-489.
38. Xu D, Zapol P, Stephenson GB, Thompson C. Kinetic Monte Carlo simulations of GaN homoepitaxy on c- and m-plane surfaces. *J. Chem. Phys.* 2017; 146(14):144702.
39. Blochl PE. Projector Augmented-Wave Method. *Phys. Rev. B.* 1994; 50(24):17953-17979.
40. Kresse G, Hafner J. Abinitio Molecular-Dynamics for Liquid-Metals. *Phys. Rev. B.* 1993; 47(1):558-561.

41. Yamamoto K, Kobayashi K, Kawanowa H, Souda R. Difference in the outermost layer between TaB₂ (0001) and HfB₂(0001). *Phys. Rev. B.* 1999; 60(23):15617-15620.
42. Epelbaum VA, Gurevich MA. On Zr-B phase diagram: Formation of ZrB₂ phase. *Zh. Fiz. Khim.* 1958; 32:2274.
43. Henkelman G, Uberuaga BP, Jonsson H. A climbing image nudged elastic band method for finding saddle points and minimum energy paths. *J. Chem. Phys.* 2000; 113(22):9901-9904.
44. Novell-Leruth G, Valcarcel A, Clotet A, Ricart JM, Perez-Ramirez J. DFT characterization of adsorbed NH_x species on Pt(100) and Pt(111) surfaces. *J Phys Chem B.* 2005; 109(38):18061-18069.
45. Novell-Leruth G, Valcarcel A, Perez-Ramirez J, Ricart JM. Ammonia dehydrogenation over platinum-group metal surfaces. Structure, stability, and reactivity of adsorbed NH_x species. *J Phys Chem C.* 2007; 111(2):860-868.
46. Walkosz W, Zapol P, Stephenson GB. A DFT study of reaction pathways of NH₃ decomposition on InN (0001) surface. *J Chem Phys.* 2012; 137(5):054708.
47. Huang WY, Lai WZ, Xie DQ. First-principles study of decomposition of NH₃ on Ir(100). *Surf. Sci.* 2008; 602(6):1288-1294.

Table and Figure Captions

Table 1. Calculated binding energies (*BEs*) of different species on the Zr-terminated (0001) surface of ZrB₂.

Figure 1. Side (first column) and top (second column) views of the Zr-terminated (0001) surface of ZrB₂ with the adsorbed (a) NH₃ (b) NH₂ (c) NH (d) N (e) H in a (2×2) surface unit cell. Zr, B, N, and H atoms represented by green, grey, and orange spheres, respectively.

Figure 2. Reaction pathway for ammonia decomposition by H abstraction on the ZrB₂(0001) surface. The (•) in the labels means that atoms are co-adsorbed in the same (2×2) surface unit cell, while (+) refers to the co-adsorption at large separation (without lateral interactions).

Table 1

Species	Site	BE (eV)	Bond lengths (Å)	H-N-H Angle (°)
NH ₃	Zr	-0.95	N-Zr: 2.38 N-H: 1.03, 1.03, 1.03	109.21, 109.21, 109.21
NH ₂	Hollow	-4.30	N-Zr: 2.34, 2.42, 2.42 N-H: 1.04, 1.05	102.66
NH	Hollow	-6.78	N-Zr: 2.22, 2.22, 2.22	--
N	Hollow	-2.72	N-Zr: 2.10, 2.10, 2.10	--
H	Hollow	-1.14	H-Zr: 2.15, 2.15, 2.15	--

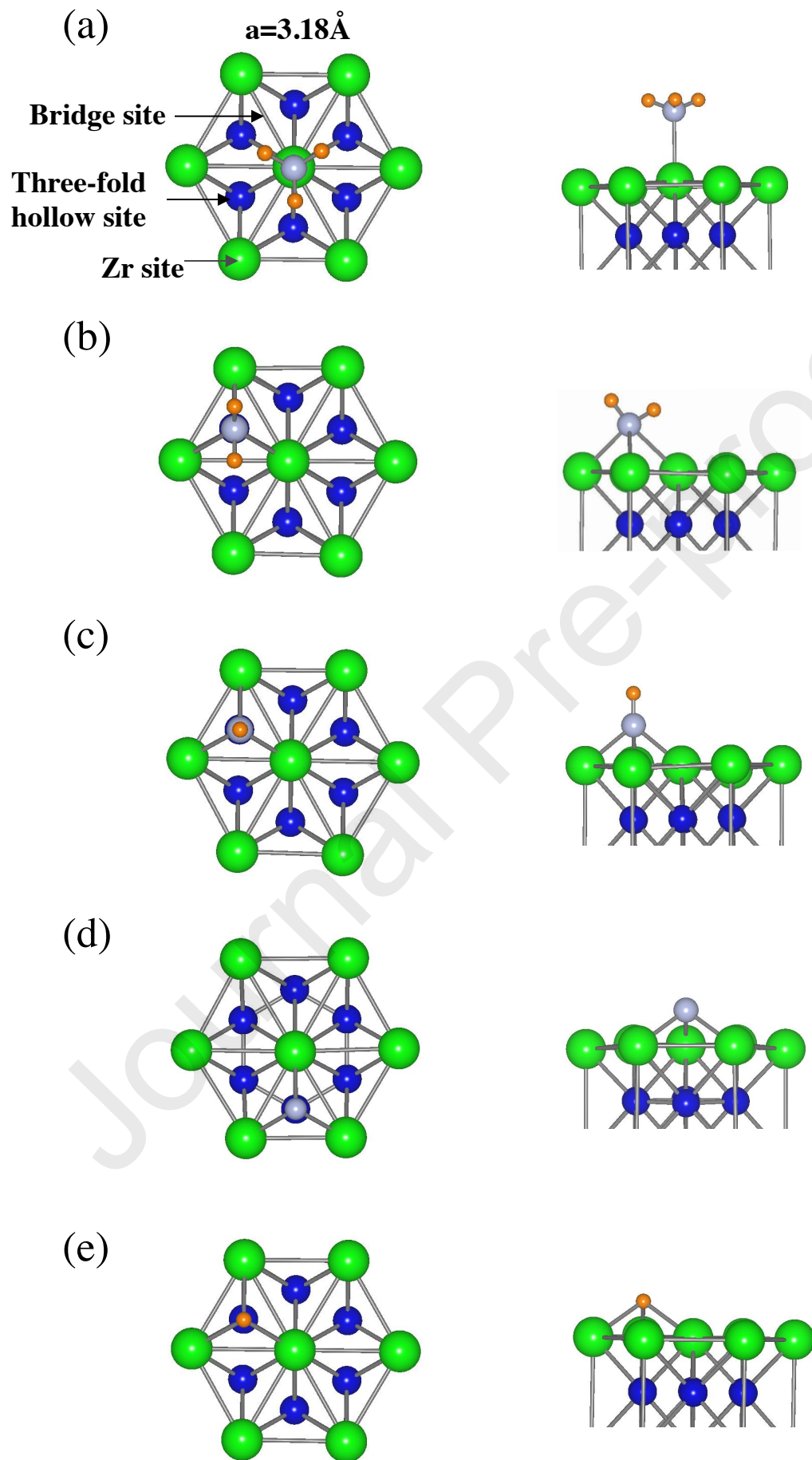
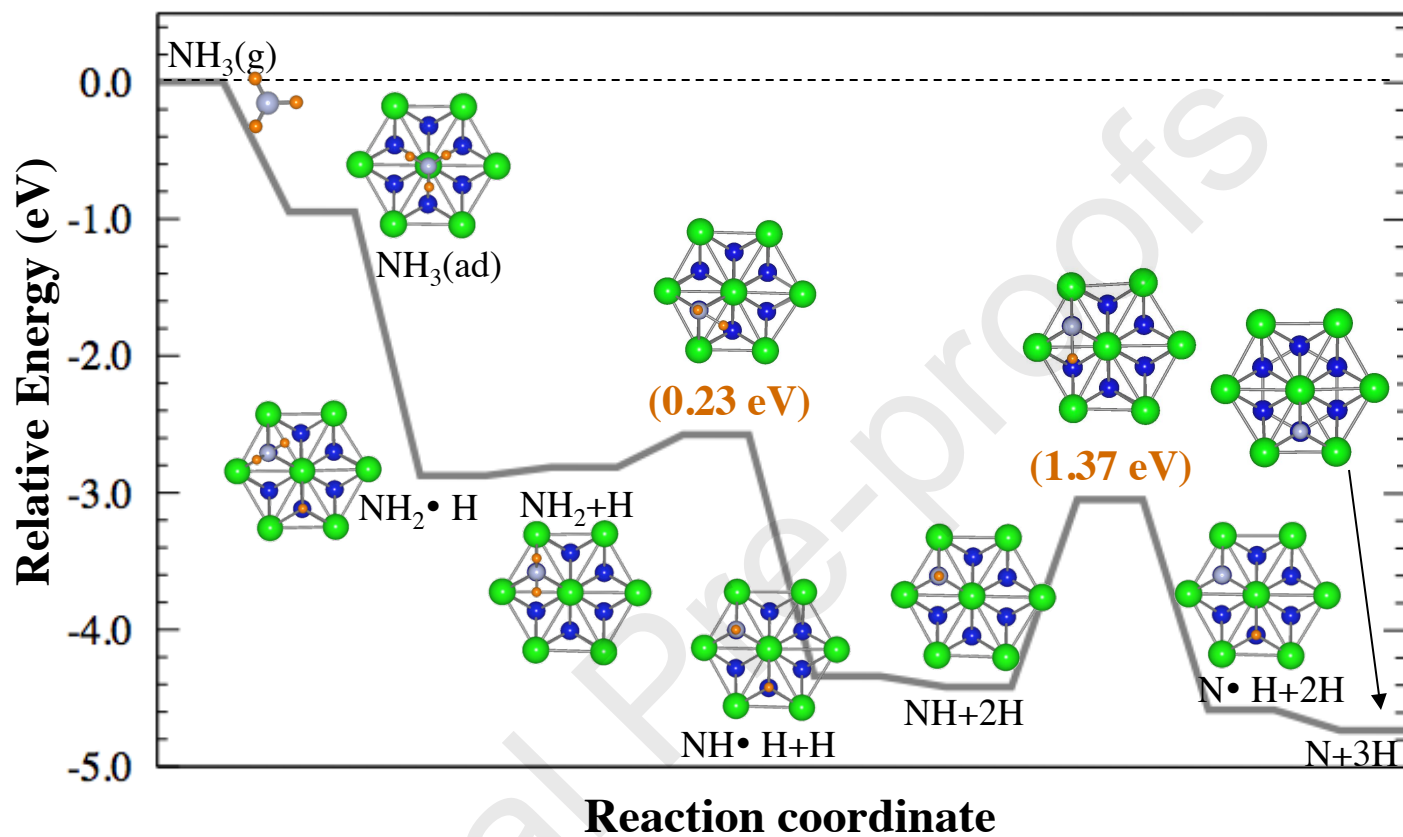
Figure 1

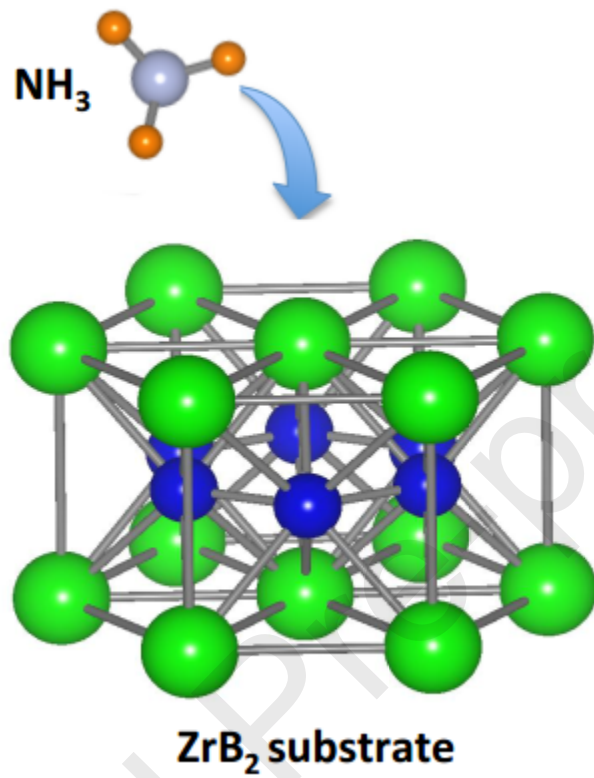
Figure 2



Highlights

- ZrB₂ is a substrate for the growth of Group-III nitrides using NH₃
- NH₃ readily adsorbs onto the Zr-site of the ZrB₂ (0001) surface
- NH₃ dissociates to atomic N and H with relatively small activation barriers
- The decomposition moieties (NH₂, NH, N and H) are very mobile on the surface

Graphical abstract



Author's contributions

WW carried out the computational work and drafted the manuscript.

WW, PZ, MT, and KM conceived the study and discussed the results. All authors read and approved the final manuscript.

Journal Pre-proofs